Catalysis Today xxx (xxxx) xxx–xxx

Contents lists available at ScienceDirect

Catalysis Today

journal homepage: www.elsevier.com/locate/cattod

Low-temperature oxidative coupling of methane using alkaline earth metal oxide-supported perovskites

Seoyeon Lim[a,b], Jae-Wook Choi[a], Dong Jin Suh[a,c], Ung Lee[a], Kwang Ho Song[b,c], Jeong-Myeong Ha[a,c,d,*]

[a] Clean Energy Research Center, Korea Institute of Science and Technology, Seoul 02792, Republic of Korea
[b] Department of Chemical and Biological Engineering, Korea University, Seoul 02841, Republic of Korea
[c] Graduate School of Energy and Environment (Green School), Korea University, Seoul 02841, Republic of Korea
[d] Division of Energy and Environment Technology, KIST School, Korea University of Science and Technology, Seoul 02792, Republic of Korea

ARTICLE INFO

Keywords:
Oxidative coupling
Methane
Perovskite
Barium oxide
Low temperature
Alkaline-earth metal oxide

ABSTRACT

Perovskite-supported alkaline-earth metal oxide catalysts were prepared for application in the oxidative coupling of methane (OCM). The selective production of C_{2+} compounds, including ethane, ethylene, acetylene, propane, and propylene, was observed at reaction temperatures < 700 °C. This lower reaction temperature was not achieved with pure perovskites but only with the combination of alkaline-earth metal oxides and perovskite supports. The formation of complex mixed oxides, such as Ba-Ca-Ti-O_x, Ba-Sr-Ti-O_x, and Ba_2TiO_4, was also observed for these catalysts. This contributed to the improved C_{2+} yield at the lower reaction temperature. The strong basicity, which contributes to the improved OCM activity, was also observed for these catalysts.

1. Introduction

Methane, as a major component of natural gas, shale gas, and gas hydrates, is an abundant hydrocarbon resource, which can be converted into valuable chemicals by both direct and synthesis-gas-based indirect chemical processes [1]. For example, although the oxidative coupling of methane (OCM) for the direct conversion of methane to olefins and paraffins has been studied for decades [2], economically feasible processes have yet to be developed. More specifically, selective OCM catalysts must be developed to produce C_{2+} compounds, including ethane, ethylene, acetylene, propane, and propylene, and reliable processes must also be designed.

Among the various catalysts reported for the OCM, perovskites (described as ABO_3 where A denotes a lanthanide, alkaline, or alkaline-earth metal, and B denotes a transition metal) have been suggested [3–5]. Although pure perovskites can be used for the OCM [3,6], perovskites modified with additives have also been prepared to improve the OCM activity. For example, $SrTiO_3$ modified with lanthanides including Nd, Pr, and Sm, or with alkaline earth metals such as Ba and Ca, exhibited improved C_{2+} selectivities of up to ~60 %, while $SrTiO_3$ modified with transition metals (Fe, Ni, Mn, and Co) preferentially formed CO and CO_2 [5]. Furthermore, the addition of metals to perovskites, where the additives partially substitute cations originally present in the perovskites [7–17], may produce electronic defects [18,19] and structural changes [20,21], thereby altering the catalytic activity. Other OCM catalysts such as Na_2WO_4/Mn [22–30], samarium oxides [31–33], and Li/MgO [34] have also been reported. In particular, Na_2WO_4/Mn/SiO_2, one of the most popular OCM catalysts, exhibits a 60–80 % C_2 selectivity at high reaction temperatures of 800–900 °C.

The objective of this study is to prepare perovskite catalysts modified by the addition of alkaline-earth metal oxides. The synergistic effects between perovskites and alkaline-earth metal oxides were reported [35], as has the influence of the support on the OCM activity [34,36–41], where perovskites ($CaTiO_3$, $SrTiO_3$, and $BaTiO_3$) prepared by the modified Pechini method [42,43] were utilized as active support materials, and alkaline-earth metal oxides (CaO, SrO, and BaO) were added by means of an impregnation method.

2. Material and methods

2.1. Catalyst preparation

Ethylene glycol ($HOCH_2CH_2OH$, 99.8 %) was purchased from Daejung (Seoul, Korea). Strontium nitrate ($Sr(NO_3)_2$, 99 %), barium nitrate ($Ba(NO_3)_2$, 99 %), calcium nitrate tetrahydrate ($Ca(NO_3)_2{\cdot}4H_2O$,

* Corresponding author at: Clean Energy Research Center, Korea Institute of Science and Technology, Seoul 02792, Republic of Korea.
E-mail address: jmha@kist.re.kr (J.-M. Ha).

https://doi.org/10.1016/j.cattod.2019.11.014
Received 30 June 2019; Received in revised form 9 November 2019; Accepted 13 November 2019

99 %), and titanium(IV) isopropoxide ($Ti(OCHCH_3CH_3)_4$, 97 %) were purchased from Sigma Aldrich (Milwaukee, Wisconsin, USA). Citric acid ($C_6H_6O_8$, 99.5 %) was purchased from Alfa Aesar (Haverhill, Massachusetts, USA). All chemicals were used as received without any further purification. Deionized (DI) water (18.2 MΩ cm) was prepared using an aquaMAX-Ultra 370 series water purification system (YL Instruments, Anyang, Korea). For the preparation of $SrTiO_3$, $BaTiO_3$, and $CaTiO_3$, titanium isopropoxide (7.6 mL) was dissolved in ethylene glycol (22.4 mL) and stirred at 60 °C for 30 min. DI water (20 mL) was added to the solution of titanium isopropoxide and ethylene glycol, which was stirred at 80 °C for a further 1 h. After this time, citric acid (19.3 g) was added to the solution at 80 °C to give a transparent-yellow solution under vigorous stirring. Subsequently, $Sr(NO_3)_2$ (5.3 g), $Ba(NO_3)_2$ (6.6 g), and $Ca(NO_3)_2{\cdot}4H_2O$ (6.0 g) were added, and after stirring for 15 h, a viscous gel was formed. This gel was then dried under air at 250 °C for no less than 24 h, and the resulting dry powder was calcined under air at 900 °C for 8 h. For the supported catalysts, calcined samples of $SrTiO_3$, $BaTiO_3$, and $CaTiO_3$ (2 g each) were added to DI water (15 mL) and under vigorous stirring at 30 °C, solutions of $Sr(NO_3)_2$ (0.41 g), $Ba(NO_3)_2$ (0.34 g), and $Ca(NO_3)_2{\cdot}4H_2O$ (0.84 g) in DI water (5 mL) were added drop-wise to the previous mixture over 10 min. The prepared solution was stirred for 2 h then dried at 105 °C for no less than 4 h to remove excess water. Finally, the resulting dried powder was calcined under air at 900 °C for 8 h prior to performing the catalytic reaction.

2.2. Catalyst characterization

Powder X-ray diffraction (XRD) was performed using a Shimadzu XRD-6000 instrument (Tokyo, Japan) with a Cu $K\alpha_1$ source ($\lambda = 1.54056$ Å). O_2-temperature programmed desorption (O_2-TPD) and CO_2-temperature programmed desorption (CO_2-TPD) were performed using a BELCAT-B catalyst analyzer (BEL Japan, Inc.) equipped with a thermal conductivity detector (TCD) and a mass spectrometer. O_2-pulse injection was also performed on the BELCAT-B analyzer. To quantify the amount of oxygen adsorbed on the surface at a reaction temperature of 675 °C, pre-calcined samples were heated to 675 °C under a flow of He, and a 5 % mixture of O_2/He was pulse-injected into the sample. X-ray photoelectron spectroscopy (XPS) was performed using a Theta Probe AR-XPS system (Thermo Fisher Scientific) with monochromated Al Kα excitation ($h\nu$ = 1486.6 eV) operated at 15 kV and 150 W at the Korea Basic Science Institute (Busan, Korea). The measured binding energy was calibrated using the C 1s peak at 284.6 eV.

2.3. Catalysis

The catalytic performances of the supported catalysts were determined using a continuous flow reaction system under ambient pressure. For this purpose, the catalyst powder (0.18 mL) was placed in the middle of a quartz reactor (height 370 mm, I.D. 6 mm) and the catalyst bed was surrounded by quartz wool for support. The remaining free space was filled with zirconia beads, which are inactive for the conversion of methane under the conditions employed herein. The catalyst bed was pretreated under nitrogen (N_2) gas at 600 °C for 40 min prior to the OCM reaction. A gas mixture of methane (CH_4), oxygen (O_2), and nitrogen (N_2) was introduced to the reactor after passing through a mixer, and the total flow of this gas mixture was fixed at 30 mL/min, corresponding to a gas-hourly space velocity (GHSV) of 10,000 h^{-1} determined at 30 °C and 1 bar pressure. Catalysis was performed under a gas mixture of $(CH_4)/(O_2)/(N_2)$ = 3/1/1 (mol/mol/mol). The reaction system was heated to 625, 650, 675, 700, and 725 °C in a stepwise manner then isothermally maintained at this temperature for 50 min. The water vapor produced during the reaction was removed by means of a cold trap (−2 °C), and the dry gas products leaving the reactor were analyzed using a 6890A gas chromatography system (Agilent Technologies, US) equipped with a flame-ionization detector (FID) and a thermal conductivity detector (TCD). The obtained products, namely methane, ethane, ethylene, acetylene, propane, and propylene, were quantified using the FID with a GS-GASPRO column (320 μm × 60 m). Oxygen, nitrogen, carbon monoxide, and carbon dioxide were quantified using the TCD with a 60/80 carboxen-1000 column. To evaluate the catalytic performance of the methane coupling reaction, the methane conversion (%), C_{2+} selectivity (%), CO_x selectivity (%), and C_{2+} yield (%) were employed as follows:.

$$CH_4 \text{ conversion } (\%) = \frac{(\text{moles of } CH_4 \text{ consumed})}{(\text{moles of } CH_4 \text{ in the feed})} \times 100$$

Selectivity to compound i

$$(S_i, \%) = \frac{(\text{number of carbon atoms per compound i molecule}) \times (\text{moles of compound i})}{(\text{moles of } CH_4 \text{ consumed})} \times 100$$

$$C_{2+} \text{ selectivity } (\%) = \frac{2 \times (\text{moles of } C_2 \text{ hydrocarbons}) + 3 \times (\text{moles of } C_3 \text{ hydrocarbons})}{(\text{moles of } CH_4 \text{ consumed})} \times 100$$

$$CO_x \text{ selectivity } (\%) = \frac{(\text{moles of CO}) + (\text{moles of } CO_2)}{(\text{moles of } CH_4 \text{ consumed})} \times 100$$

$$C_{2+} \text{ yield } (\%) = \frac{(CH_4 \text{ conversion}) \times (C_{2+} \text{ selectivity})}{100}$$

3. Results and discussion

3.1. Oxidative coupling of methane (OCM) over perovskites

Prior to preparation of the modified perovskites, the catalytic process was performed using pure perovskites, including $CaTiO_3$ (CTO), $SrTiO_3$ (STO), and $BaTiO_3$ (BTO), to demonstrate the poor OCM activity of these perovskite catalysts at temperatures < 700 °C (Fig. 1 and Table S1). More specifically, CTO appears inactive in the production of C_{2+} hydrocarbons but more active for the production of CO and CO_2 via deep oxidation (Fig. 1). Interestingly, CTO exhibited a CO selectivity two times higher than that of CO_2 (Table S1). Because of the poor OCM activity and the higher selectivity to CO (requiring 1.5 O_2 molecules for the conversion of CH_4 to CO and H_2O) over CO_2 (requiring 2 O_2 molecules for the conversion of CH_4 to CO_2 and H_2O), only 49.9 % of the O_2 was consumed at 725 °C. Increasing the reaction temperature improved the OCM activity to increase the CH_4 conversion, O_2 conversion, and C_{2+} selectivity. In the case of STO, the supplied oxygen was essentially consumed at temperatures > 700 °C. Indeed, upon increasing the reaction temperature from 700 to 725 °C, a slightly decreased methane conversion and significantly increased C_{2+} selectivity were observed, thereby exhibiting an increased C_{2+} yield. Furthermore, BTO exhibited an improved C_{2+} selectivity upon increasing the reaction temperature above 650 °C, and its methane and oxygen conversions also increased in a similar manner. Moreover, the C_{2+} yield of BTO increased significantly from 6.9–15.0% upon increasing the reaction temperature from 700 to 725 °C.

3.2. Oxidative coupling of methane (OCM) over the alkaline-earth metal oxide (CaO, SrO, and BaO) supported perovskites

Although STO and BTO required a minimum reaction temperature of approximately 700 °C to achieve any appreciable OCM activity, the deposition of alkaline-earth metal oxides (CaO, SrO, and BaO) on these perovskites improved the OCM activity at temperatures < 700 °C (Fig. 2 and Table S2). The methane conversion and C_{2+} selectivity also increased for these supported perovskite catalysts upon increasing the reaction temperature. More specifically, BaO/STO and BaO/CTO

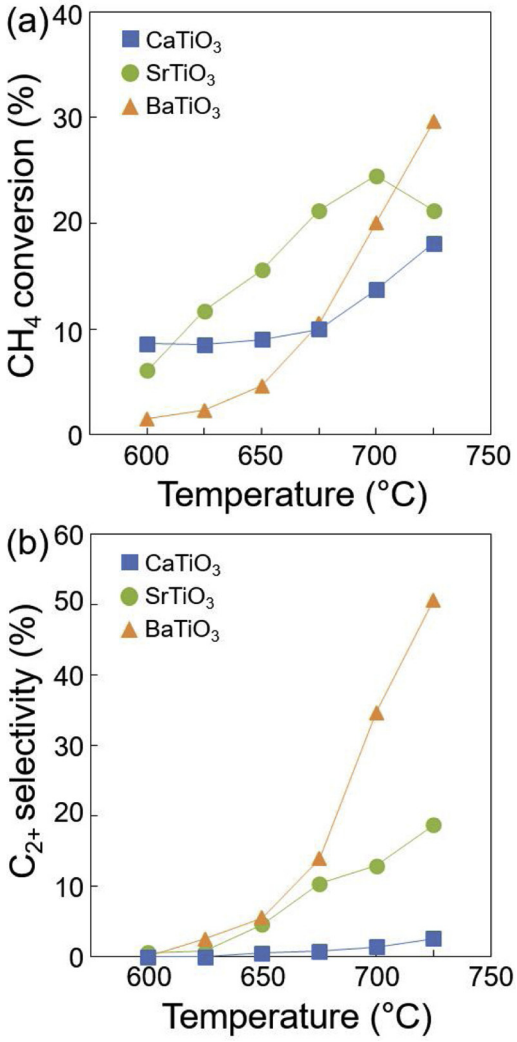

Fig. 1. Effects of reaction temperature on (a) CH_4 conversions and (b) C_{2+} selectivities obtained using the $CaTiO_3$ (CTO), $SrTiO_3$ (STO), and $BaTiO_3$ (BTO) perovskite catalysts. The GHSV was 10,000 h^{-1} and the methane-to-oxygen (CH_4/O_2) ratio was fixed at 3 (mol/mol).

(orange circles and squares in Fig. 2, respectively) exhibited methane conversions > 24 % at 625 and 650 °C, respectively. Their corresponding C_{2+} yields were 10.1 % (BaO/CTO) and 10.0 % (BaO/STO) at 650 °C. In contrast, SrO/CTO and CaO/STO exhibited lower C_{2+} yields (5.1 and 9.3 %, respectively) even at the higher temperature of 675 °C. We note that all supported catalysts consumed almost 100 % of the O_2 provided and exhibited C_{2+} yields > 13 % at 700 °C, which indicates that the addition of alkaline-earth metal oxides improved the OCM activity compared to corresponding unsupported perovskites, and the observed OCM activities of these catalysts should be examined at temperatures < 700 °C for catalyst screening.

Among the various catalysts examined in this study, BaO-deposited perovskites (BaO/CTO and BaO/STO) exhibited higher C_{2+} yields (10.1 and 10.0 %, respectively) at 650 °C. To confirm the effects of BaO on the OCM activity, BaO-deposited fumed silica (BaO/SiO_2) and $Na_2WO_4/Mn/SiO_2$ (BaO/NWM) were prepared using the same procedure employed for preparation of the supported perovskites as described in the Supplementary data. SiO_2 was selected as an inert support in the case of BaO/SiO_2, and $Na_2WO_4/Mn/SiO_2$ (NWM) was selected as an active non-perovskite catalyst in the case of BaO/NWM. Thus, BaO/SiO_2 was found to be OCM-inactive over a range of temperatures (600–725 °C, Fig. S1), while BaO/NWM was unsuitable for the low-temperature OCM, exhibiting a 6.0 % C_{2+} yield at 725 °C. Because NWM alone

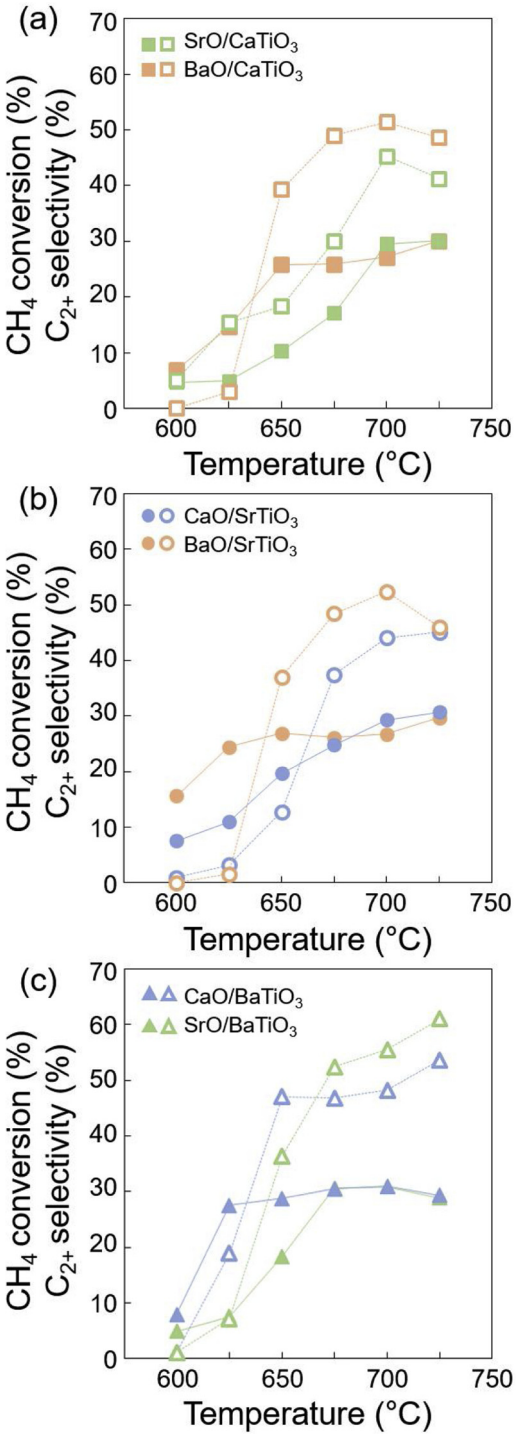

Fig. 2. CH_4 conversions and C_{2+} selectivities of (a) the supported $CaTiO_3$ (CTO), (b)the supported $SrTiO_3$ (STO), and (c) the supported $BaTiO_3$ (BTO GHSV was 10,000 h^{-1} and the methane-to-oxygen (CH_4/O_2) ratio was fixed at 3 (mol/mol). Filled and empty symbols (squares, circles, and triangles) indicate the CH_4 conversion and C_{2+} selectivity, respectively.

exhibited a 7.2 % C_{2+} yield at 725 °C, the activity of BaO/NWM could not be attributed to the presence of BaO, and the synergy between BaO and NWM could be ignored. These observations indicate that BaO itself (i.e., in the absence of perovskites) did not exhibit noticeable C_{2+} hydrocarbon production, and so it was apparent that the synergistic effects between the alkaline-earth metal oxides (in particular BaO) and the perovskites improved the OCM activity.

We also found that supported BaO catalysts and BTO-based catalysts

exhibited high OCM activities at low reaction temperatures (i.e., < 700 °C). In addition to the supported BaO catalysts discussed above, Ba-containing perovskite-based catalysts also exhibited good OCM activities (triangles in Fig. 2). The highest catalytic activities were therefore observed for SrO/BTO and CaO/BTO, particularly in the temperature ranges of 675–700 and 625–650 °C, respectively, with a 5.2 % C_{2+} yield being obtained for CaO/BTO at 625 °C.

Moreover, Ba-free catalysts were found to exhibit higher CO selectivities (c.f., CO_2 production) at 700 °C although poor OCM activities were observed, particularly for CaO/STO and SrO/CTO (Table S2). The other Ba-containing catalysts preferentially formed CO_2 over CO, and the CO selectivities of CaO/STO and SrO/CTO were 3.1 and 2.4 times higher than those of the other supported catalysts at 675 °C, respectively.

The roles of the Ba species were further observed using Ba-doped CTO ($Ba_{0.2}Ca_{0.8}TiO_3$) or STO ($Ba_{0.2}Sr_{0.8}TiO_3$) catalysts which were prepared using a modified Pechini method [5], as described in the Supplementary data. The C_{2+} yields obtained using these catalysts were 2.1 % ($Ba_{0.2}Sr_{0.8}TiO_3$) and 9.5 % ($Ba_{0.2}Ca_{0.8}TiO_3$) at 725 °C, thereby indicating lower OCM activities compared to the supported perovskites. Interestingly, the Ba-doped CTO, which exhibited the higher C_{2+} yield, formed the $BaTiO_3$ (PDF# 05-0626) structure along with the $CaTiO_3$ (PDF# 42-0423) structure, while the Ba-doped STO formed only the $SrTiO_3$ (PDF# 35-0734) structure (Fig. S2). These observations indicate that the formation of Ba-containing mixed oxides may indeed improve the OCM activity.

3.3. XRD

Following XRD examination of the roles of Ba or Ba oxides in the catalytic OCM reaction (Fig. S2), the crystal structures of the catalysts were further correlated with the OCM activity, and it was found that the complex non-perovskite mixed oxides formed by the combination of deposited alkaline earth metals and perovskites may improve the OCM activity (Fig. 3). Prior to observing the supported catalysts, the crystal structures of the CTO, STO, and BTO perovskites, which were poor OCM catalysts (Fig. 1), were observed, and the formation of $SrTiO_3$ (PDF# 35-0734), $BaTiO_3$ (PDF# 05-0626), and $CaTiO_3$ (PDF# 42-0423) perovskites confirmed for STO, BTO, and CTO, respectively (Fig. 3). In addition, the BaO-deposited perovskites, i.e., BaO/STO and BaO/CTO, which exhibited higher OCM activities, were found to contain no BaO structure but rather new phases, including $Ba_{1.91}Sr_{0.09}TiO_4$ (PDF# 13-0522) and $BaCaTiO_4$ (PDF# 38-1481), thereby indicating the facile deposition of barium onto STO and CTO. In these catalysts, absence of the BaO structure indicates the formation of well-dispersed Ba species or the incorporation of Ba into perovskite supports. Note that a generic metal oxide "BO" mixed with an alkali metal oxide or alkaline earth metal oxide "AO" can form various oxide phases (AO, A_2O, BO), mixed oxides (A_2BO_3), or carbonates on the surface [44]. As discussed in the previous section, it is interesting that the Ba-doped $CaTiO_3$, prepared using the modified Pechini method [5] with an atomic ratio of (Ba + Ca)/(Ti) = 1 (atom/atom), formed $CaTiO_3$ (PDF# 42-0423) and $BaTiO_3$ (PDF# 05-0626), while the Ba-doped $SrTiO_3$ prepared according to the same method formed $SrTiO_3$ (PDF# 35-0734) rather than any non-perovskite structures, which differs from those of the supported perovskites (Fig. S2). In addition to the BaO-deposited perovskites, CaO/BTO was found to contain non-perovskite structures, including barium calcium titanium oxide ($BaCaTiO_4$, PDF# 13-0323), without any trace of the CaO structure being observed. Because of the smaller radius of calcium (180 pm) compared to strontium (200 pm) and barium (215 pm), the incorporation of calcium into BTO can be favored. Moreover, the addition of SrO to BTO was found to cause a partial phase transition of the perovskite into a layered perovskite, namely barium orthotitanate (Ba_2TiO_4, PDF# 38-1481), as reported for Mg, Ca, and Ba-substituted $SrTiO_3$ exhibiting two phases of cubic perovskites and tetragonal layered perovskites [8]. In contrast to the Ba-containing catalysts, the barium-free catalysts (i.e., CaO/STO and SrO/CTO), which exhibited lower OCM activities, were found to contain deposited alkaline-earth metal (CaO (PDF# 37-1497) and perovskite supports ($CaTiO_3$ and $SrTiO_3$) without any new phases. These observations suggest that the formation of complex mixed oxides or the strong interactions between alkaline-earth metal oxides and perovskites were likely responsible for the improved OCM activities observed for

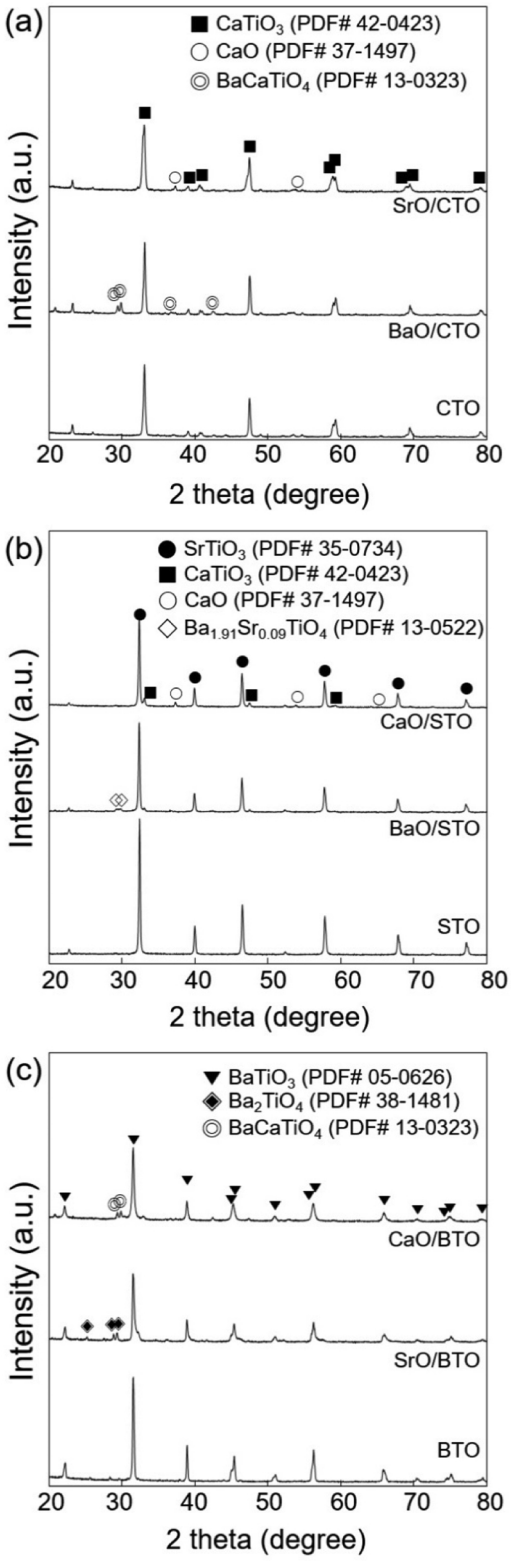

Fig. 3. XRD results for the (a) CTO-, (b) STO-, and (c) BTO-based catalysts.

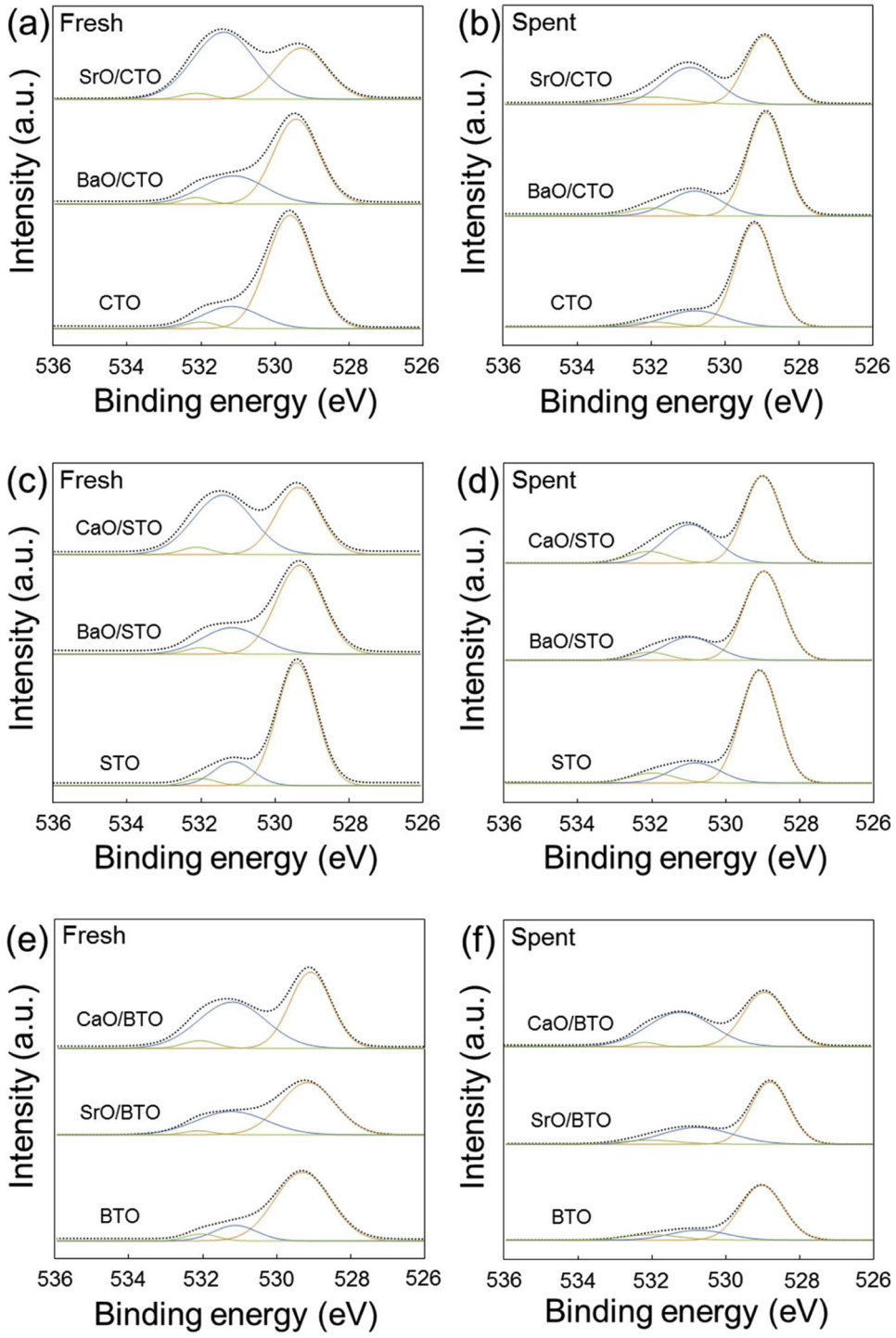

Fig. 4. O 1s XPS results for the fresh and spent (a, b) CTO-, (c,d) STO-, and (e,f) BTO-based catalysts.

these species. When the catalytic activity was correlated with the XRD results, the catalysts composed of Ba-containing complex mixed oxides, such as $Ba_{1.91}Sr_{0.09}TiO_4$ and $BaCaTiO_4$, exhibited higher OCM activities (i.e., 10.1–13.5 % C_{2+} yields at 650 °C) compared to those containing only alkaline earth metal oxides and perovskites. As discussed in the context of the XRD results, Ba oxides were not observed for any of the Ba-containing catalysts, thereby indicating that the synergy between alkaline earth metal oxides and perovskites must improve the OCM activity.

Upon increasing the reaction temperature to 725 °C, CaO/BTO and SrO/BTO gave 15.7 and 17.6 % yields of C_{2+}, respectively, and new phases were also observed, namely $BaCaTiO_4$ and Ba_2TiO_4, respectively. In addition, upon measurement of the bulk structures of the spent catalysts, the formation of barium carbonate ($BaCO_3$, PDF# 05-0378) and calcium carbonate ($CaCO_3$, PDF# 01-0837) was confirmed for the majority of these catalysts as the complex mixed oxides (e.g., barium-calcium and barium-strontium titanates) disappeared (Fig. S3) [21]. It should also be noted there that only CaO/BTO exhibited the carbonate-free $BaTiO_3$ structure.

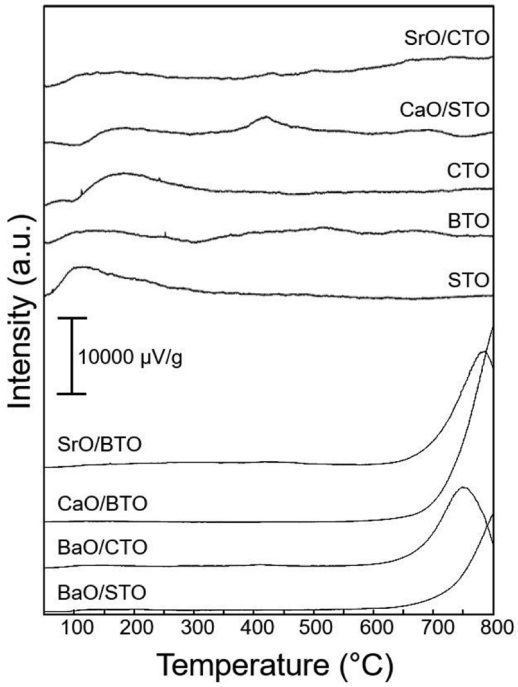

Fig. 5. CO_2-TPD results for the perovskite catalysts.

3.4. XPS

The relationship between the surface oxygen species (lattice oxygen atoms, peroxides, superoxides, carbonates, and hydroxyl groups) and the catalytic OCM activity was then investigated further using XPS (Fig. 4 and Table S3). It was found that the larger fraction of surface lattice oxygen species compared to that of surface adsorbed oxygen species improved the OCM activity for the alkaline earth metal oxide-supported perovskites. However, this was not the case for the perovskites because of the different compositions of the catalysts. As indicated in Fig. 4, the O 1s peaks could be deconvoluted into O_{lat} lattice oxygen atoms (529.0–529.7 eV), O_{ads} surface-adsorbed oxygen atoms (531.0–531.2 eV), and CO_3^{2-} carbonate species (531.3–532.0 eV). All supported catalysts were found to contain trace amounts of carbonates (CO_3^{2-}), while the Ca-containing catalysts exhibited larger C 1s peaks corresponding to CO_3^{2-} at approximately 289 eV (Fig. S4). For the O 1s spectra of the fresh perovskites (i.e., CTO, STO, and BTO), large O_{lat}/O_{ads} ratios were observed (Table S3), which increased after the OCM reaction, thereby indicating the consumption of surface-adsorbed oxygen species. Furthermore, freshly prepared supported alkaline earth metal oxides exhibited lower ratios of O_{lat}/O_{ads} compared to the perovskites, and the reduction in these values after the OCM reaction indicated a reduced consumption of surface-adsorbed oxygen atoms. Among the supported alkaline-earth metal oxide catalysts examined herein, the supported BaO catalysts, i.e., BaO/CTO and BaO/STO, exhibited larger O_{lar}/O_{ads} ratios. We note that both SrO/CTO and CaO/STO, which exhibited smaller O_{lat}/O_{ads} ratios, gave higher CO selectivities and lower C_{2+} selectivities compared to the other catalysts (Fig. 2 and Table S2).

3.5. Temperature-programmed desorption of oxygen and carbon dioxide (O_2-TPD and CO_2-TPD)

For an improved understanding of the oxygen species involved in the catalytic process, the catalysts were subjected to O_2-temperature programmed desorption (O_2-TPD) and O_2-pulse injection methods (Fig. S5 and Table S4). In the case of O_2-TPD, no appreciable O_2 desorption peaks were observed (Fig. S5), and no reliable correlation between O_2 desorption and the catalytic activity was obtained. Indeed, O_2-pulse injection indicated that only CTO, a poor OCM catalyst, demonstrated an O_2 adsorption of 0.03 cm^3/g, which was 4–6 times larger than those of the other catalysts (Table S4). We note that larger quantities of adsorbed oxygen species were also observed for the poor OCM catalysts described in our previous study [35].

As depicted in Fig. 5, a greater surface basicity improved the low temperature OCM activity, as confirmed by CO_2-TPD [41]. BaO-deposited and BTO-supported catalysts, which exhibited good OCM activities, demonstrated a strong basicity, although BTO exhibited negligible CO_2 desorption peaks up to 800 °C. This was also reported in terms of an improved surface basicity upon the addition of alkaline and alkaline-earth metal oxides [45,46] and the associated improvement in the OCM activity [47,48]. In addition, the combination of Ba and Ca (or Sr) exhibited a large quantity of desorbed CO_2. When BaO was deposited on the fumed silica (BaO/SiO_2) and NWM catalysts (BaO/NWM), little or no surface basicity was observed (Fig. S6). Furthermore, from the OCM results obtained at 650 °C, the C_{2+} yield of BTO, which exhibited a low surface basicity, was 0.2 %, while the yields for BaO/CTO and BaO/STO, which exhibited high surface basicity values, were 10.1 and 10.0 %, respectively. Moreover, the yields obtained for CaO/BTO and SrO/BTO, which exhibited high surface basicity values, were 14.3 and 16.1 % at 675 °C, respectively, while the yield obtained for BTO was only 1.5 %.

4. Conclusion

The low temperature oxidative coupling of methane (OCM) activities of perovskites ($CaTiO_3$ (CTO), $SrTiO_3$ (STO), and $BaTiO_3$ (BTO)) and alkaline-earth metal (CaO, SrO, BaO)-deposited perovskites were observed at 600–725 °C. It was found that catalysts containing complex mixed oxide structures such as barium calcium titanium oxide or barium-strontium titanium oxide, which formed because of the strong interactions between alkaline earth metal oxides and the perovskite supports, exhibited improved OCM activities. More specifically, BaO/CTO, BaO/STO, and CaO/BTO gave C_{2+} yields of 10–13.5 % at 650 °C. Upon increasing the reaction temperature to 725 °C, the SrO/BTO-forming barium orthotitanate (Ba_2TiO_4) exhibited the best OCM results, i.e., a C_{2+} yield of 17.6 %. This improved catalytic activity was attributed to the strong surface basicity as determined by CO_2-temperature-programmed desorption measurements, in addition to the formation of complex mixed oxides (barium-calcium titanium oxide, barium-strontium titanium oxide, or barium orthotitanate) comprising of the deposited oxides and the supports, as confirmed by X-ray diffraction studies. These results are expected to be of relevance as the development of selective OCM catalysts for the production of C_{2+} compounds in an economically feasible lower temperature process is necessary to convert methane into valuable chemicals.

CRediT authorship contribution statement

Seoyeon Lim: Investigation, Writing - original draft. **Jae-Wook Choi:** Methodology, Investigation. **Dong Jin Suh:** Conceptualization, Funding acquisition. **Ung Lee:** Data curation. **Kwang Ho Song:** Supervision. **Jeong-Myeong Ha:** Conceptualization, Writing - review & editing, Supervision.

Declaration of Competing Interest

The authors declare that there are no conflicts of interest.

Acknowledgements

This work was supported by C1 Gas Refinery Program through the National Research Foundation of Korea (NRF) funded by the Ministry of Science and ICT. (2015M3D3A1A01064900).

Appendix A. Supplementary data

Supplementary material related to this article can be found, in the online version, at doi:https://doi.org/10.1016/j.cattod.2019.11.014.

References

[1] W. Taifan, J. Baltrusaitis, Appl. Catal. B 198 (2016) 525–547.
[2] G.E. Keller, M.M. Bhasin, J. Catal. 73 (1982) 9–19.
[3] I. Kim, G. Lee, H.B. Na, J.-M. Ha, J.C. Jung, Mol. Catal. 435 (2017) 13–23.
[4] S.G. Li, N.P. Xu, J. Shi, M.Z.C. Hu, E.A. Payzant, J. Mater. Sci. Lett. 20 (2001) 1631–1633.
[5] S. Lim, J.-W. Choi, D.J. Suh, K.H. Song, H.C. Ham, J.-M. Ha, J. Catal. 375 (2019) 478–492.
[6] G. Lee, I. Kim, I. Yang, J.-M. Ha, H.B. Na, J.C. Jung, Appl. Surf. Sci. 429 (2018) 55–61.
[7] K. Nomura, T. Hayakawa, K. Takehira, Y. Ujihira, Appl. Catal. A Gen. 101 (1993) 63–72.
[8] D.V. Ivanov, L.A. Isupova, E.Y. Gerasimov, L.S. Dovlitova, T.S. Glazneva, I.P. Prosvirin, Appl. Catal. A Gen. 485 (2014) 10–19.
[9] D. Neagu, J.T.S. Irvine, Chem. Mater. 23 (2011) 1607–1617.
[10] X.P. Xiang, L.H. Zhao, B.T. Teng, J.J. Lang, X. Hu, T. Li, Y.A. Fang, M.F. Luo, J.J. Lin, Appl. Surf. Sci. 276 (2013) 328–332.
[11] W.P. Ding, Y. Chen, X.C. Fu, Appl. Catal. A Gen. 104 (1993) 61–75.
[12] M.J. Lee, J.H. Jun, J.S. Jung, Y.R. Kim, S.H. Lee, Bull. Korean Chem. Soc. 26 (2005) 1591–1596.
[13] Y. Teraoka, T. Nobunaga, N. Yamazoe, Chem. Lett. (1988) 503–506.
[14] R. Spinicci, P. Marini, S. De Rossi, M. Faticanti, P. Porta, J. Mol. Catal. A-Chem. 176 (2001) 253–265.
[15] H. Imai, T. Tagawa, N. Kamide, J. Catal. 106 (1987) 394–400.
[16] A. Sato, S. Ogo, Y. Takeno, K. Takise, J.G. Seo, Y. Sekine, ACS Omega 4 (2019) 10438–10443.
[17] Z. Fakhroueian, F. Farzaneh, N. Afrookhteh, Fuel 87 (2008) 2512–2516.
[18] H.Y. Zhu, P.F. Zhang, S. Dai, ACS Catal. 5 (2015) 6370–6385.
[19] L. Liu, D.D. Taylor, E.E. Rodriguez, M.R. Zachariah, Chem. Commun. 52 (2016) 10369–10372.
[20] M.A. Pena, J.L.G. Fierro, Chem. Rev. 101 (2001) 1981–2017.
[21] D. Kwon, I. Yang, Y. Sim, J.-M. Ha, J.C. Jung, Catal. Commun. 128 (2019) 105702.
[22] S. Arndt, T. Otremba, U. Simon, M. Yildiz, H. Schubert, R. Schomacker, Appl. Catal. A Gen. 425 (2012) 53–61.
[23] U. Simon, O. Gorke, A. Berthold, S. Arndt, R. Schomacker, H. Schubert, Chem. Eng. J. 168 (2011) 1352–1359.
[24] S.-B. Li, Chin. J. Chem. 19 (2001) 16–21.
[25] S. Gu, H.S. Oh, J.W. Choi, D.J. Suh, J. Jae, J. Choi, J.M. Ha, Appl. Catal. A Gen. 562 (2018) 114–119.
[26] X. Fang, S. Li, J. Lin, Y. Chu, J. Mol. Catal. (China) 6 (1992) 427–433.
[27] R.T. Yunarti, S. Gu, J.-W. Choi, J. Jae, D.J. Suh, J.-M. Ha, ACS Sustain. Chem. Eng. 5 (2017) 3667–3674.
[28] J.Y. Lee, W. Jeon, J.-W. Choi, Y.-W. Suh, J.-M. Ha, D.J. Suh, Y.-K. Park, Fuel 106 (2013) 851–857.
[29] J. Wang, L. Chou, B. Zhang, H. Song, J. Zhao, J. Yang, S. Li, J. Mol. Catal. A Chem. 245 (2006) 272–277.
[30] S. Gu, H.-S. Oh, J.-W. Choi, D.J. Suh, J. Jae, J. Choi, J.-M. Ha, Appl. Catal. A Gen. 562 (2018) 114–119.
[31] L. Mleczko, M. Baerns, Fuel Process. Technol. 42 (1995) 217–248.
[32] T.W. Elkins, H.E. Hagelin-Weaver, Appl. Catal. A Gen. 454 (2013) 100–114.
[33] J.S. Yoon, Y.H. Kim, E.J. Lee, M.J. Ji, B.H. Choi, H.J. Hwang, Electron. Mater. Lett. 7 (2011) 209–213.
[34] T. Ito, J.H. Lunsford, Nature 314 (1985) 721–722.
[35] Y. Gambo, A.A. Jalil, S. Triwahyono, A.A. Abdulrasheed, J. Ind. Eng. Chem. 59 (2018) 218–229.
[36] U. Zavyalova, M. Holena, R. Schlogl, M. Baerns, ChemCatChem 3 (2011) 1935–1947.
[37] K. Kwapien, J. Paier, J. Sauer, M. Geske, U. Zavyalova, R. Horn, P. Schwach, A. Trunschke, R. Schlogl, Angew. Chem. Int. Ed. 53 (2014) 8774–8778.
[38] T. Ito, J.X. Wang, C.H. Lin, J.H. Lunsford, J. Am. Chem. Soc. 107 (1985) 5062–5068.
[39] J. Song, Y. Sun, R. Ba, S. Huang, Y. Zhao, J. Zhang, Y. Sun, Y. Zhu, Nanoscale 7 (2015) 2260–2264.
[40] B.M. Sollier, L.E. Gomez, A.V. Boix, E.E. Miro, Appl. Catal. A Gen. 532 (2017) 65–76.
[41] V.R. Choudhary, B.S. Uphade, S.A.R. Mulla, Ind. Eng. Chem. Res. 36 (1997) 3594–3601.
[42] E.R. Leite, J.A. Varela, E. Longo, C.A. Paskocimas, Ceram. Int. 21 (1995) 153–158.
[43] D. Segal, J. Mater. Chem. 7 (1997) 1297–1305.
[44] E.E. Wolf, J. Phys. Chem. Lett. 5 (2014) 986–988.
[45] V.R. Choudhary, S.A.R. Mulla, B.S. Uphade, Ind. Eng. Chem. Res. 37 (1998) 2142–2147.
[46] H.L. Wan, X.P. Zhou, W.Z. Weng, R.Q. Long, Z.S. Chao, W.D. Zhang, M.S. Chen, J.Z. Luo, S.Q. Zhou, Catal. Today 51 (1999) 161–175.
[47] J.W. Xu, Y. Zhang, Y.M. Liu, X.Z. Fang, X.L. Xu, W.M. Liu, R.Y. Zheng, X. Wang, Eur. J. Inorg. Chem. (2019) 183–194.
[48] C.Q. Chu, Y.H. Zhao, S.G. Li, Y.H. Sun, Phys. Chem. Chem. Phys. 18 (2016) 16509–16517.